

# Supramolecular Oligothiophene Microfibers Spontaneously Assembled on Surfaces or Coassembled with Proteins inside Live Cells

Giovanna Barbarella<sup>\*,†</sup> and Francesca Di Maria<sup>†,‡</sup>

<sup>†</sup>Consiglio Nazionale Ricerche (CNR-ISOF), Via P. Gobetti 101, I-40129 Bologna, Italy

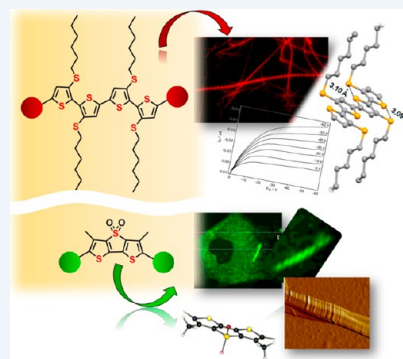
<sup>‡</sup>Dipartimento di Matematica e Fisica “Ennio De Giorgi”, Università del Salento, via Monteroni, I-73100 Lecce, Italy

**CONSPECTUS:** During the last few decades, multifunctional nano- and microfibers made of semiconducting  $\pi$ -conjugated oligomers and polymers have generated much interest because of a broad range of applications extending from sensing to bioelectronic devices and (opto)electronics.

The simplest technique for the fabrication of these anisotropic supramolecular structures is to let the molecules do the work by spontaneous organization driven by the information encoded in their molecular structure.

Oligothiophenes—semiconducting and fluorescent compounds that have been extensively investigated for applications in thin-film field-effect transistors and solar cells and to a lesser extent as dyes for fluorescent labeling of proteins, DNA, and live cells—are particularly suited as building blocks for supramolecular architectures because of the peculiar properties of the thiophene ring. Because of the great polarizability of sulfur outer-shell electrons and the consequent facile geometric deformability and adaptability of the ring to the environment, thiophene can generate multiple nonbonding interactions to promote non-covalent connections between blocks. Furthermore, sulfur can be hypervalent, i.e., it can accommodate more than the eight electrons normally associated with s and p shells. Hypervalent oligothiophene-S,S-dioxides whose oxygen atoms can be involved in hydrogen bonding have been synthesized. These compounds are amphiphilic, and some of them are able to spontaneously cross the membrane of live cells. Hypervalent nonbonding interactions of divalent sulfur, defined as weak coordination to a proximate nitrogen or oxygen, have also been invoked in the solid-state packing of many organic molecules and in the architecture of proteins.

In this Account, we describe two different types of thiophene-based building blocks that can induce the spontaneous formation of nanostructured microfibers in very different environments. The first, based on the synthesis of “sulfur-overrich” hexamers and octamers, leads to surface-independent self-assembly of microfibers—helical or rodlike depending on the groups attached to the same identical inner core—that are crystalline, fluorescent, and conductive and display chirality despite the lack of chiral carbon atoms on the building blocks. Supramolecular polymorphic microfibers are also formed, and they are characterized by very different functional properties. The second, based on a rigid oligothiophene-S,S-dioxide, leads to coassembled protein–oligothiophene microfibers that are physiologically formed inside live cells. The oligothiophene-S,S-dioxide can indeed spontaneously cross the membrane of live cells and be directed toward the perinuclear region, where it is recognized and incorporated by specific peptides during the formation of fibrillar proteins without being harmful to the cells. Coassembled oligothiophene–protein microfibers are progressively formed through a cell-mediated physiological process. Thanks to the oligothiophene blocks, the microfibers possess fluorescence and charge-conduction properties. By means of fluorescence imaging, we demonstrated that various types of live cells seeded on these microfibers were able to internalize and degrade them, experiencing in turn different effects on their morphology and viability, suggesting a possible use of the microfibers as multiscale biomaterials to direct cell behavior. On the whole, our results show the great versatility of oligothiophene building blocks and allow us to foresee that their capabilities of spontaneous assembly in the most different environments could be exploited in much more exciting research fields than those explored to date.



## ■ INTRODUCTION

There is a wide range of literature concerning nano/microfibers made of  $\pi$ -conjugated oligomers and polymers, the investigations spanning from preparation and characterization to technological applications in medical devices, (opto)electronics, biosensors, and smart textiles.<sup>1,2</sup> Anisotropic structures such as microfibers may display better chemical and physical properties and hence better device performance than their bulk counter-

parts. For example, according to a recent study on charge transport over multiple length scales in supramolecular microfiber transistors, the charge mobility in single fibers is multiple orders of magnitude higher than in thin-film devices, demonstrating the great potential of supramolecular ordered

Received: April 30, 2015

Published: August 3, 2015

Scheme 1. Oligothiophenes Forming Microfibers on Surfaces ( $R = C_6H_{13}$ ); The Red Dashed Lines Indicate the Intramolecular S...S Nonbonding Interactions Present in the Inner Quaterthiophene Core, As Revealed by the Single-Crystal X-ray Structure of Compound 2<sup>24</sup>

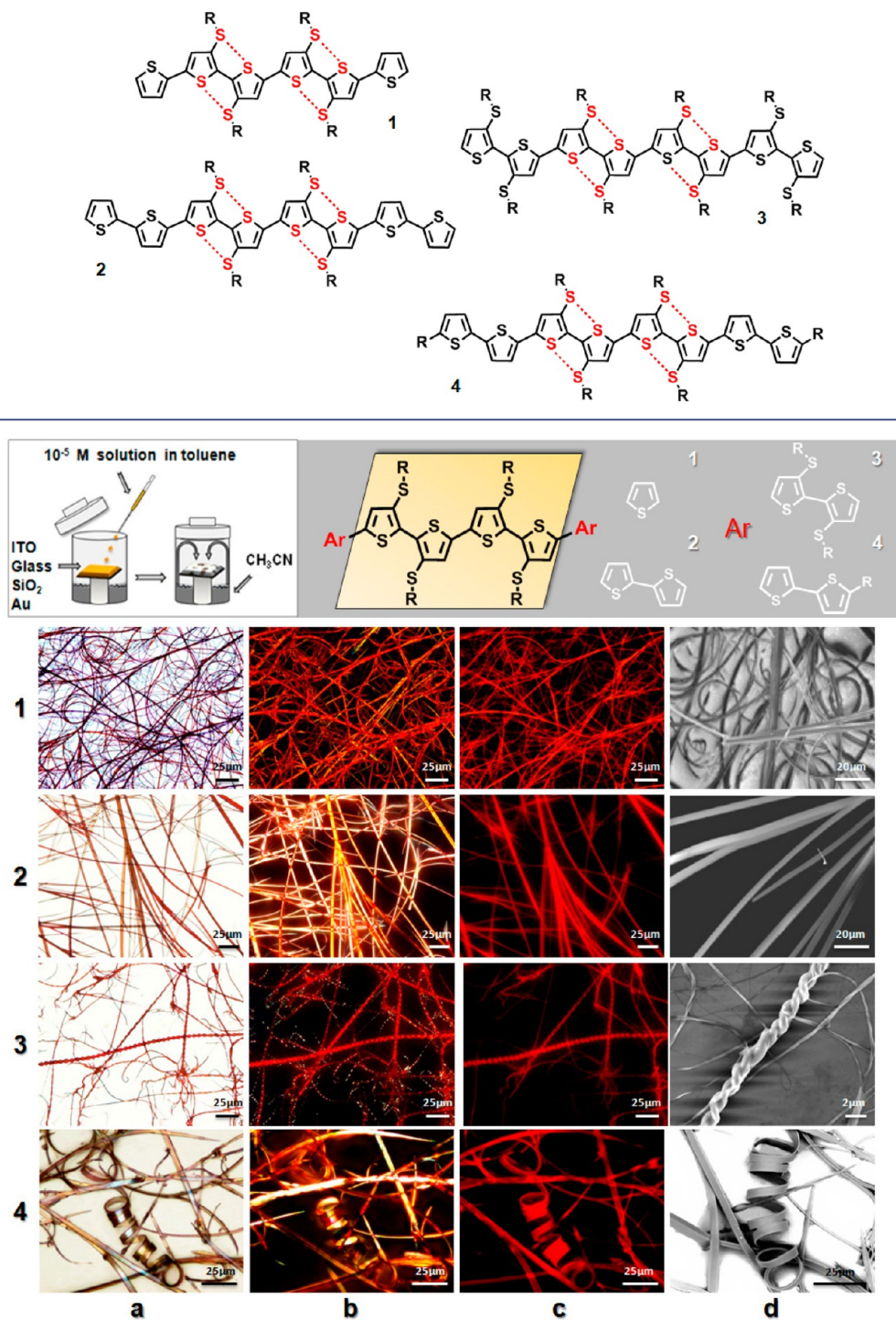


**Figure 1.** (a, b) Optical microscopy images (a) without and (b) with crossed polarizers, (c) fluorescence microscopy images, and (d) scanning electron microscopy images of representative microfibers formed on glass by compounds 1–4.  $R = C_6H_{13}$ . Adapted from ref 24. Copyright 2011 American Chemical Society.

microfibers for device applications.<sup>3</sup> Different methods for the production of functional nano/microfibers have been investigated, ranging from template-directed preparation to electrospinning and nanolithography.<sup>1</sup> One of the simplest and most studied “bottom-up” methods is solution-processed self-assembly, which involves the generation of complex architec-

tures from modular molecular blocks through nonbonding interactions without direction by outside forces.<sup>1,4–6</sup> A great variety of  $\pi$ -conjugated systems have been explored, including thiophene oligomers, which are monodisperse fluorescent and semiconducting compounds made of a limited number of  $\alpha$ -linked (or, less often,  $\alpha,\beta$ - or  $\beta$ -linked) thiophene rings.<sup>7,8</sup> The

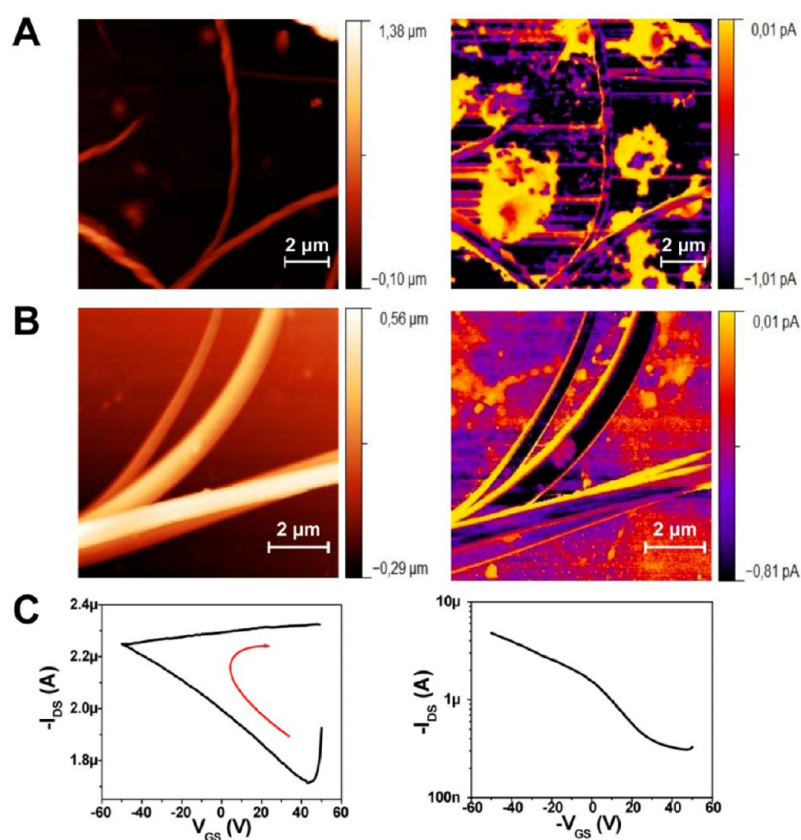


**Figure 2.** (A, B) Topography images (left) and hole transportation measurements (right) of helical fibers of (A) 3 and (B) 2 grown on ITO obtained by the Tr-TUNA technique. (C) Transfer characteristics in the saturation regime in air for bottom-contact field-effect transistors with active layers made of microfibers of (left) 3 and (right) 2 directly grown on the device. Reproduced from ref 24. Copyright 2011 American Chemical Society.

self-assembly into microfibers of a few oligothiophenes functionalized with biomolecules has been described.<sup>9–11</sup>

The presence of sulfur confers two peculiar characteristics to the thiophene ring compared with other five-membered-ring heterocycles. First, because of the large sizes of the 3s and 3p orbitals, sulfur outer-shell electrons are easily polarizable and available for multiple nonbonding interactions. As a consequence, the thiophene ring can alter its shape to adapt to varying environmental conditions and become geometrically irregular, as shown by single-crystal X-ray structures in which thiophene never displays the same geometrical features.<sup>12</sup> The geometrical adaptability of thiophene to the environment is helped by the facile conformational interchangeability of oligothiophenes due to low energy differences between rotational isomers and low energy barriers to conformational interconversion.<sup>13</sup> Single-crystal X-ray diffraction analysis has revealed that the self-assembly modalities of oligothiophenes are driven by van der Waals interactions,  $\pi$ - $\pi$  stacking, and a variety of anisotropic directional donor-acceptor intra- and intermolecular C-H $\cdots$ S, C-H $\cdots$ O, C-H $\cdots$  $\pi$ , and S $\cdots$ S interactions.<sup>14</sup> Significant nonbonded interactions between divalent sulfur and aromatic rings have also been reported.<sup>15</sup> Second, sulfur can be hypervalent, i.e., its surrounding electrons may exceed the number of eight normally associated with completely filled s and p subshells.<sup>16,17</sup> Hypervalent nonbonding interactions, defined as weak coordination of a divalent sulfur to O, N, or S, have been invoked in the solid-state packing of organic molecules and protein structure.<sup>18</sup> Hypervalency enables the functionalization of thiophene sulfur with

oxygen atoms, as in oligo- and polythiophene-S,S-dioxides, which display very peculiar electrical and optical properties.<sup>19,20</sup>

The presence of oxygen generates numerous hydrogen-bonding interactions in the single-crystal X-ray structures of oligothiophene-S,S-dioxides<sup>21,22</sup> to add to the numerous nonbonding interactions mentioned above.

Our challenge was to exploit the versatility of the thiophene ring<sup>23</sup> to develop chemical strategies for the spontaneous formation of ordered micrometric supramolecular structures on surfaces and in a completely different environment such as that of living cells. Indeed, the micrometric scale is not only the useful dimension of currently investigated electronic devices but also corresponds to the size of live cells. On the basis of the directionality of S $\cdots$ S and hydrogen-bonding interactions, empirical design led us to synthesize “sulfur-overrich” oligothiophenes<sup>24</sup> and rigid oligothiophene-S,S-dioxides<sup>25</sup> as building blocks that can induce the formation of anisotropic, ordered, supramolecular systems in the micrometric regime. In this Account we describe, on one side, how the first type of building block leads to the self-assembly of crystalline supramolecular microfibers having the same characteristics independent of the deposition surface and additional properties inherent to the organization into microfibers. On the other, we describe how the second type of building block can spontaneously cross the membrane of live cells and coassemble inside them with specific fibrillar proteins. The process does not cause any harm to the cells and leads to the physiological formation of microfibers that are fluorescent and capable of charge transport.

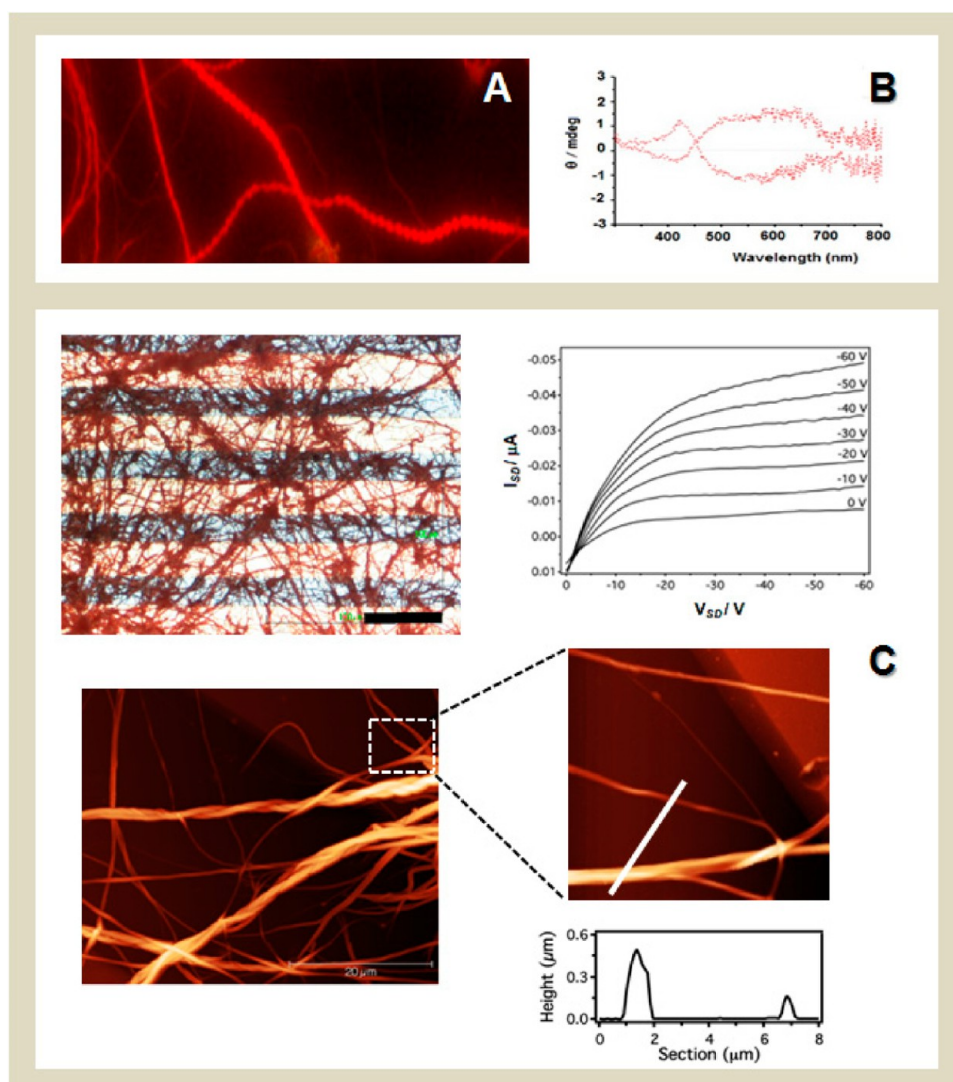


**Figure 3.** (A) Fluorescence microscopy image and (B) CD spectra of the red microfibers of **3** grown on glass. (C) AFM images and profiles and  $I$ – $V$  output of the red microfibers of **3** directly grown on the  $\text{SiO}_2$  surface of a bottom-contact field-effect transistor. Adapted with permission from ref 31. Copyright 2014 Wiley-VCH Verlag GmbH.

### ■ MICROFIBERS SPONTANEOUSLY ASSEMBLED ON SURFACES

We generated crystalline microfibers by exploiting the directionality of  $\text{S}\cdots\text{S}$  nonbonding interactions<sup>26</sup> for the spontaneous self-assembly of anisotropic thiophene supramolecular architectures. To this end, oligothiophenes functionalized with an extra sulfur atom at the  $\beta$  position of the thiophene ring (“sulfur-overrich” oligothiophenes) were synthesized through a newly developed synthetic platform.<sup>24</sup> Scheme 1 shows the molecular structures of these oligothiophenes, all having the same identical inner quaterthiophene core with two head-to-head junctions of the  $\text{S}$ -hexyl substituents. In this way, four possible patterns for nonbonding  $\text{S}\cdots\text{S}$  interactions (red dashed lines) were created. The single-crystal X-ray structure of compound **2** showed that the inner quaterthiophene core is strictly planar—which facilitates the stacking arrangement in the solid state—with short  $\text{S}\cdots\text{S}$  intramolecular distances of 3.09 and 3.10 Å.<sup>27,24</sup>

We found that only the quaterthiophene with this precise regiochemistry promotes the formation of microfibers, with any other arrangement of the  $\text{S}$ -hexyl groups leading invariably to

amorphous morphologies. Also, the hexyl chains were needed for the formation of microfibers, as replacement with shorter chains resulted in star-shaped crystalline aggregates. The quaterthiophene itself does not form microfibers; the microfibers are formed only when terminal aryl groups are present in the structure. In turn, the terminal aryl groups dictate the morphology of the microfibers as rodlike or folded, as illustrated in Figure 1. The quaterthiophene is a powerful building block that induces microfiber formation when terminated not only with thiophene rings but also with bromine, benzothiazole, or fluorinated/ $\text{S}$ -alkylated bithiophene, hence allowing for very fine tuning of the functional properties of the microfibers.<sup>28</sup>

Figure 1 reports a sketch illustrating the conditions for the formation of the microfibers on various types of surfaces. A few drops of the oligothiophenes dissolved at room temperature in toluene, a solvent in which they are very soluble, were deposited on the surface of choice on a solid support inside a glass cylinder containing at the bottom acetonitrile, a solvent in which they are poorly soluble. The drops of oligomers in toluene diffused on the substrate, and when the acetonitrile

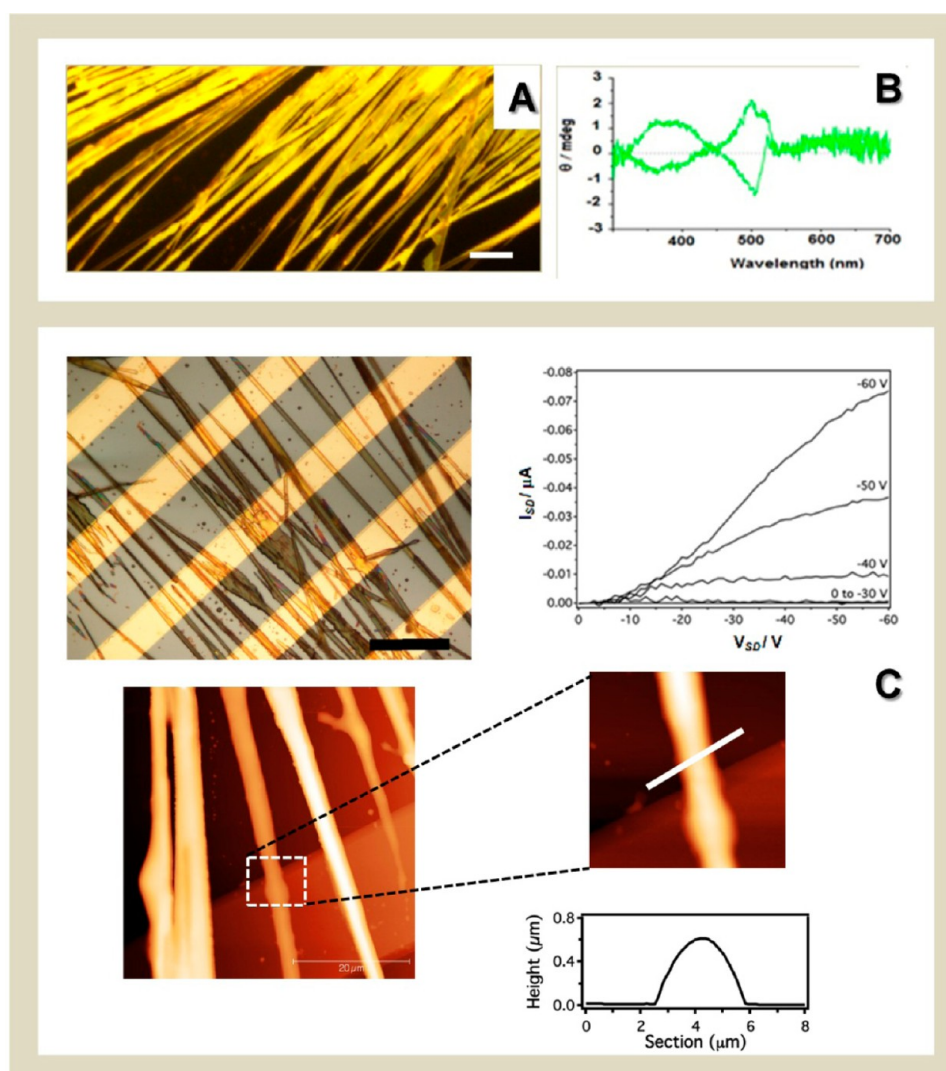


**Figure 4.** (A) Fluorescence microscopy image and (B) CD spectra of the yellow microfibers of **3** grown on glass. (C) AFM images and profiles and  $I$ – $V$  output of the yellow microfibers of **3** directly grown on the  $\text{SiO}_2$  surface of a bottom-contact field-effect transistor. Adapted with permission from ref 31. Copyright 2014 Wiley-VCH Verlag GmbH.

vapors came in contact with them, crystallization in the form of microfibers took place. Afterward the substrate was removed and allowed to dry on a Petri dish. With formation rates varying from a few minutes to few hours depending on the molecular structure (compound **3** was the slowest one), randomly oriented microfibers were formed. If not exposed to acetonitrile vapors, **1**–**4** always afforded globular aggregates. The microfibers, characterized by lengths of several micrometers, widths of a few micrometers, and submicrometric thickness, were reproducibly formed on glass, indium tin oxide (ITO), silicon, and gold, always with the same results.<sup>24</sup> Figure 1 shows optical microscopy images (without and with crossed polarizers) of representative microfibers formed by **1**–**4** on glass, together with fluorescence and scanning electron microscopy images. All of the microfibers displayed birefringence, being extinguished at four positions at intervals of  $90^\circ$  upon rotation of the polarized light, indicating their crystalline nature. The microfibers were redox-active, fluorescent, and conductive.<sup>24</sup> Since aggregates formed on surfaces are the result of a balance between molecule–molecule and molecule–substrate interactions, in the case of **1**–**4** the molecule–molecule interactions always prevailed, leading to stable supramolecular systems with the

same characteristics on every type of surface. Morphologically, the most interesting system was compound **3**, which formed multihelical structures where superhelices (helices of helices) or even double helices of superhelices were present, displaying left-handed or right-handed helicity with the one or the other always predominating.<sup>24</sup>

The nanoscale charge conductivity of the microfibers directly grown on ITO was measured by conductive atomic force microscopy (C-AFM) and tunneling atomic force microscopy in torsion mode (Tr-TUNA),<sup>29</sup> while the applicability in devices was tested with microfibers grown on the  $\text{SiO}_2$  surface of a field-effect transistor (FET) with gold contacts.<sup>24</sup> The results are shown in Figure 2. Figure 2A,B compares the topography images of the microfibers—helical for **3** and rodlike for **2**—and the charge transport measured by Tr-TUNA. Figure 2C shows the transfer characteristics in the saturation regime in air for bottom-contact FETs with active layers made of microfibers of **3** and **2**.<sup>24</sup> Both microfibers display p-type (hole-transporting) characteristics, in agreement with the FET charge mobility measured for the hexadecamer of **3**.<sup>30</sup>

Compound **3** generated a second type of crystalline microfibers with a different arrangement of the molecular

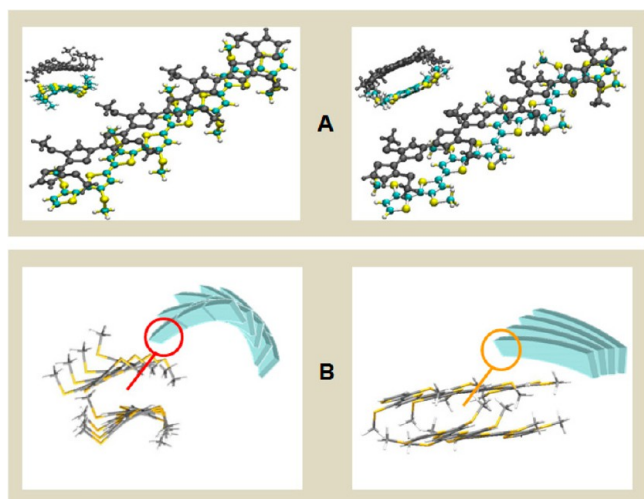


**Figure 5.** (A) Calculated preferred conformations of **3** ( $R = \text{SCH}_3$ ) and geometries of the aggregates made of two molecules. (B) Sketch of the proposed supramolecular organization of the yellow and red microfibers. Adapted with permission from ref 31. Copyright 2014 Wiley-VCH Verlag GmbH.

building blocks.<sup>31</sup> Besides crystalline red helical microfibers, crystalline yellow rodlike microfibers exhibiting different functional properties were separately and reproducibly obtained starting from polymorphic powders. Figures 3 and 4 show fluorescence images, circular dichroism (CD) spectra, and AFM images and profiles of the two supramolecular polymorphs of **3**, together with the current–voltage ( $I$ – $V$ ) output of field-effect transistors with the polymorphic microfibers directly grown on the device. Both forms exhibited p-type charge transport characteristics, with the yellow microfibers showing an FET charge mobility ( $\sim 10^{-3} \text{ cm}^2 \text{ V}^{-1} \text{ s}^{-1}$ ) and on/off current ratio ( $10^4$ ) that were 1 and 3 orders of magnitude, respectively, greater than those of the red ones. It is worth noting that the charge transport values could be improved by controlling the self-assembly of microfibers by confinement effects<sup>27</sup> and that no FET charge mobility could be measured for cast films of oligomers **1**–**4**.<sup>24</sup>

Besides charge transport, the organization in microfibers also confers on octamer **3** circular dichroism properties that are not observed in solution or in cast films since the compound lacks asymmetrically substituted carbon atoms. However, both polymorphic microfibers display circular dichroism signals with significant differences from one form to the other. For each polymorph, separately grown on glass, Figures 3B and 4B report the CD spectra of two different samples, reversed in sign. Since in the microfibers the two handednesses have equal probabilities, different samples may display opposite chiralities.<sup>31</sup>

Figure 5 illustrates the model proposed for the formation of the supramolecular polymorphs on the basis of X-ray diffraction data and theoretical calculations on conformational preferences and aggregation modalities.<sup>31</sup> In both cases the molecules are organized in platelets that form crystalline domains. In the yellow microfibers, these domains are parallel with interchain stacking and strongly  $\pi$ – $\pi$ -interacting building blocks, whereas in the red microfibers they tend to bend, forming curves and curls.

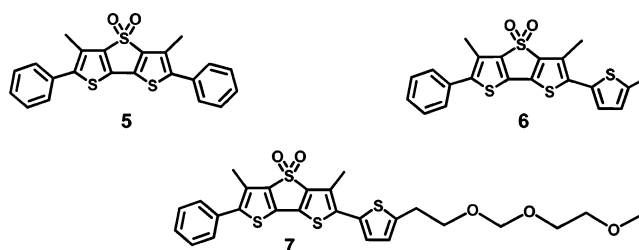
The organization in microfibers and the diversity of supramolecular forms of the same molecule expand the range

of tunability of the functional properties of conjugated materials. Although we are still unable to sufficiently control the formation of oligothiophene microfibers because they rely on a repertoire of non-covalent interactions that are poorly understood, empirical criteria based on chemical intuition and synthetic expertise allow the engineering of new molecular building blocks and hence the manipulation of relevant material parameters.

## ■ MICROFIBERS SPONTANEOUSLY COASSEMBLED WITH PROTEINS INSIDE LIVE CELLS

In the past few years, we have developed a few families of thiophene fluorophores that are optically stable and brightly

### Scheme 2. Molecular Structures of Cell-Permeant Dithienothiophene-*S,S*-dioxide (DTTO) Fluorescent Dyes That Promote the Physiological Secretion of Protein–Dye Microfibers by Live Cells



fluorescent and can successfully be employed for the labeling of proteins and DNA.<sup>32–34</sup> We have also described biocompatible thiophene fluorophores that can spontaneously penetrate the membrane of living cells and uniformly stain the cytoplasm with long-lasting fluorescence and no harm to the cells.<sup>35</sup> Moreover, we have found that some dithienothiophene-*S,S*-dioxide (DTTO) derivatives are cell-permeant fluorescent dyes that cause the secretion of fluorescent microfibers by live cells (Scheme 2).<sup>25,36,37</sup>

Compounds **5**–**7** were characterized by intense green fluorescence and high optical and chemical stability; they were cell-permeant, entering the cells predominantly by diffusion across cellular lipid bilayers,<sup>38</sup> and were not toxic to the cells.<sup>25</sup> When dissolved in physiological solution, they were spontaneously taken up by live mouse embryonic fibroblasts (NIH-3T3) and HeLa cells.<sup>25</sup> DTTO **5** was also successfully tested with bone-marrow-derived human fibroblasts (BMFBs)<sup>36</sup> and mouse neuroblastoma cells (B104).<sup>37</sup> Figure 6A shows laser scanning confocal microscopy (LSCM) images of the spontaneous uptake of **5** by BMFBs as a function of time. After the uptake (0 h), rapid and uniform fluorescent staining of the cytoplasm was evident, while the nucleus remained dark. After 3–6 h, multiple fluorescent spots were present, while after 6–9 h, fluorescent fibers started to be extruded from the cells. With time (up to 120 h), progressive accumulation of fluorescent fibers of micrometer length, submicrometric diameter, and large aspect ratios were observed, while a slight uniform fluorescent staining of the cytoplasm could still be observed.

Figure 6B shows 3D confocal scanning images of BMFB cells treated with **5** and their optical sectioning, indicating the subcell compartmentalization of the photoluminescence. The fluorescent fibers displayed a complex helical supramolecular arrangement and a periodicity of luminescence on the order of micrometers (Figure 6B, panels e and j). Confocal  $z$ -stack

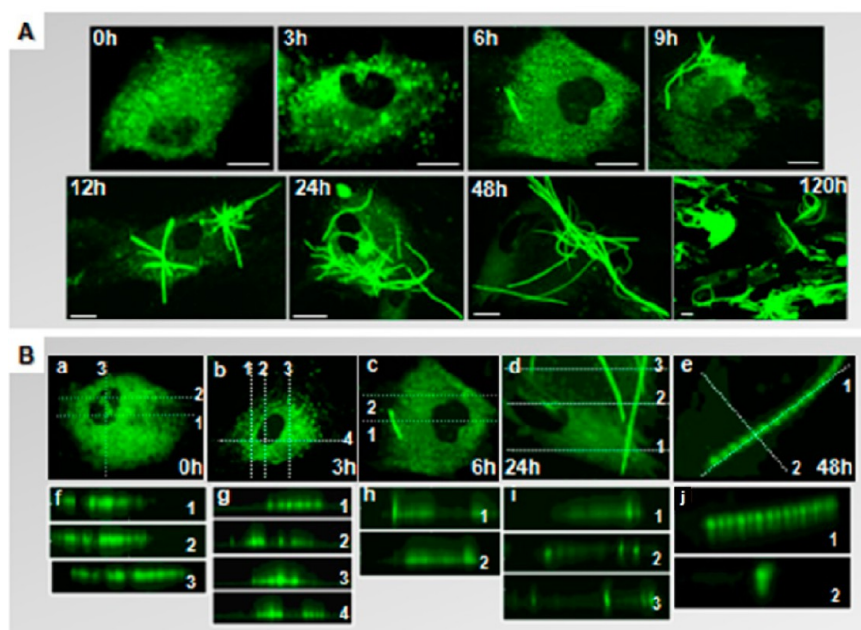


**Figure 6.** (A) LSCM images of the intracellular formation of fluorescent microfibers with time upon spontaneous uptake of **5** by bone-marrow human tumor fibroblasts (BMFBs). Independent cell cultures were examined at each time, and one or a few cells are reported as representative of the whole sample population. Scale bars: 10  $\mu\text{m}$ . (B) 3D LSCM images of fiber production by BMFBs through photoluminescence reconstruction in the  $z$  direction: (a) 0 h; (b) 3 h; (c) 6 h; (d) 24 h; (e) 48 h. The corresponding optical sections (f–j), with a  $z$  resolution of 200 nm, show that the microfibers were formed inside the cells. Adapted with permission from ref 36. Copyright 2013 Royal Society of Chemistry.

images revealed that multiple fluorescent fibers were synthesized inside the cells and then released as unique supramolecular assemblies through the cellular plasma membrane. Analogous results were obtained with **6** and **7** using mouse fibroblasts (NIH-3T3 cell line).<sup>25</sup> On the whole, our observations indicated that (a) native-cell processes guide the formation of fluorescent fibers, which do not alter cell viability; (b) the integration of synthetic **5–7** does not affect the endogenous synthesis of fibrous structures at the molecular level; and (c) the fluorescent microfibers remain cell-permeant, resembling fibroblast-mediated processing and physiological release of extracellular matrix (ECM) components through the plasma membrane. Sodium dodecyl sulfate polyacrylamide gel electrophoresis (SDS-PAGE) of the fluorescent microfibers isolated from the cell milieu, immune-blotting analysis of nitrocellulose-blotted gels with an anticollagen type-I antibody, and colocalization experiments of isolated microfibers obtained using NIH-3T3 fibroblasts with anticollagen type-I antibody allowed us to establish that the fluorescent microfibers formed by fibroblasts upon uptake of **5** were mainly made of type-I collagen.<sup>25,36</sup> Figure 7 shows (A) LSCM and (B, left) AFM images of a left-handed helical microfiber under native experimental conditions at 120 h upon uptake of **5**. The higher-magnification image (Figure 7B, middle) reveals both longitudinal and transverse periodicity of the fine structure, indicating axial periodicity of about 150–200 nm and lateral periodicity of about 70–100 nm, in agreement with the structure of type-I collagen.<sup>39</sup>

To account for our experimental results, we assumed that DTTO **5** is specifically recognized by some component of procollagen polypeptide chains at some stage of its formation and incorporated via hydrogen bonding.<sup>25,36</sup> The progressive aggregation of polypeptide chains into the triple helix then drives the simultaneous self-assembly of **5** inside the triple helix itself in a process of coassembly, leading to a unique

supramolecular fibrillar architecture that is more stable than those that would be obtained by isolated self-assembly of either building block. Theoretical calculations carried out on a system consisting of three sequences of the tripeptide Gly-Pro-HyPro (as a model for procollagen chains) in the presence of **5** support this hypothesis.<sup>25</sup> The calculations predicted an energetically favorable configuration (Figure 7C) involving a hydrogen bond between the HyPro and one of the oxygen atoms of **5**.

The periodicity of fixation of **5** through multiple hydrogen bonds, related to the presence of HyPro at regular distances in the procollagen polypeptide chains, creates periodicity in fluorescence emission on the nanometer scale. The fluorescence periodicity observed at the micrometer scale in the fibrils secreted by the cells is related to the wrapping of several nanometer-sized fluorescent fibrils into themselves. As a result of the presence of **5**, a fluorescent and semiconducting molecule,<sup>21</sup> the coassembled microfibers are fluorescent and show conductive behavior (Figure 7D).<sup>36</sup>

The ability of **5** to induce the physiological formation of fluorescent microfibers in live cells extends to other cell types and to proteins other than collagen. Figure 8A shows LSCM images of the intracellular formation of fluorescent microfibers upon treatment of mouse neuroblastoma cells (B104) with a micromolar physiological solution of **5**. The fluorophore spontaneously crossed the cell membrane, diffused into the cells, and accumulated around the perinuclear region, forming globular aggregates without penetrating the nucleus. After 24 h, the formation of fluorescent microfibers of micrometer size within the cytoplasm of several cells was apparent, and these microfibers progressively accumulated inside the cells. Many microfibers displayed details where helical green fluorescent structures were present (see the inset of Figure 8A, panel c). The fluorescent microfibers formed after 7 days from treatment with **5** were separated from the cell lysate, picked up by LSCM,

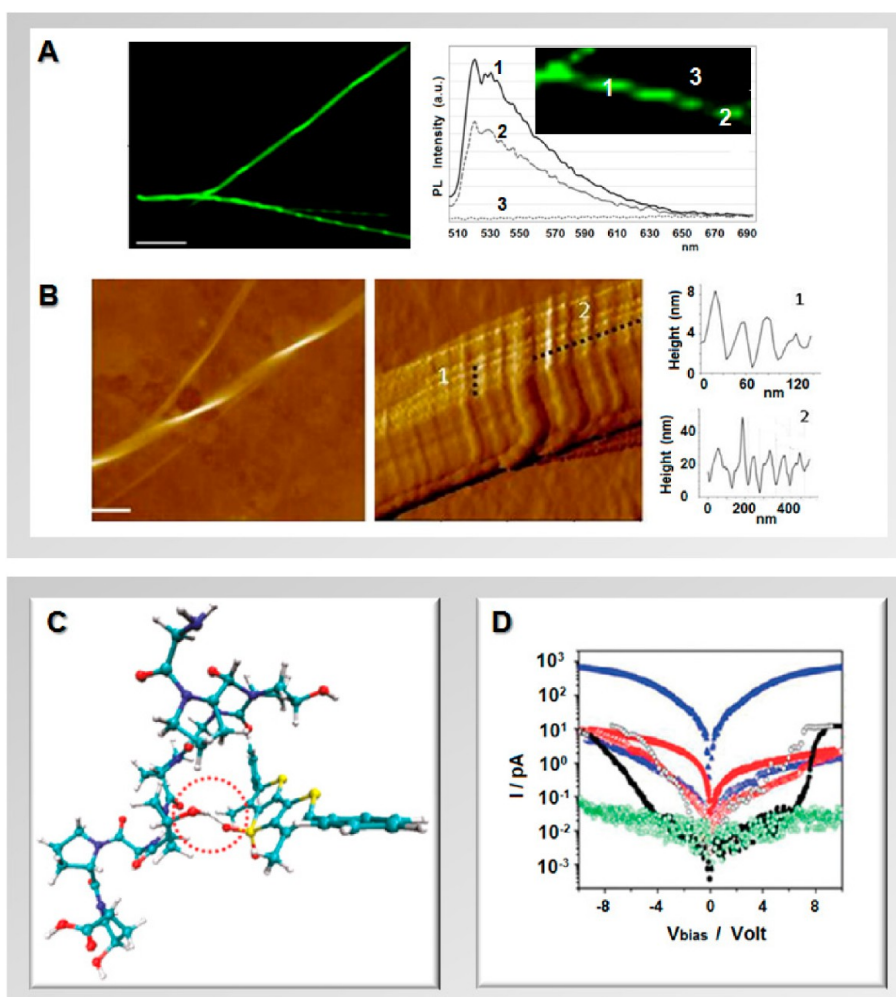


**Figure 7.** (A) LSCM and (B) noncontact AFM topography of fibers under native experimental conditions after 120 h from spontaneous uptake of **5**. The higher-magnification AFM image (B, middle) reveals both longitudinal periodicity (150–200 nm) and transverse periodicity (70–100 nm). (C) DFT-calculated “complex” of **5** with three sequences of the tripeptide glycine-proline-hydroxyproline (Gly-Pro-HyPro) as a model for a collagen strand. The circle indicates the hydrogen bond formed in the inner tripeptide between the O–H group of HyPro and the O=S=O group of the dithienothiophene core of **5**. (D) Semilogarithmic plot of the average currents calculated on 20 *I*–*V* traces for the fluorescent microfibers formed upon uptake of **5**–**7** compared with those of the dyes alone. For details, see ref 36. Scale bars: (A) 10  $\mu\text{m}$ ; (B, left) 2  $\mu\text{m}$ ; (B, middle) 200 nm. (A, B, D) Reproduced with permission from ref 36. Copyright 2013 Royal Society of Chemistry. (C) Reproduced from ref 25. Copyright 2011 American Chemical Society.

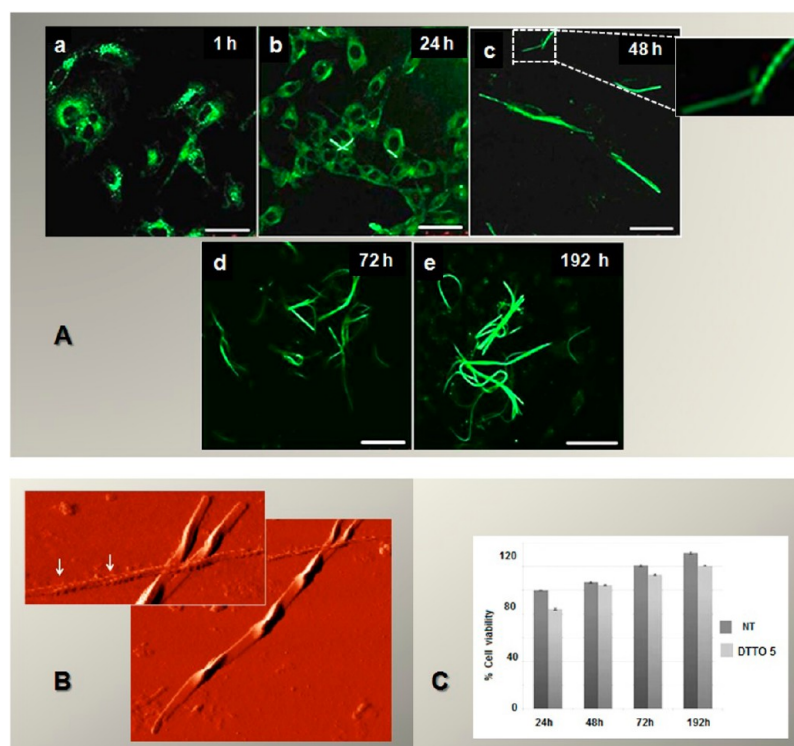
and analyzed by several techniques.<sup>37</sup> HPLC–ESI–QTof–MS analysis indicated that more than 70% of the fluorescent microfibers were made of vimentin, a protein of the intermediate filaments of the cytoskeleton characterized by the presence of  $\alpha$ -helical “rod” domains.<sup>37,40,41</sup> Colocalization experiments with the monoclonal vimentin antibody showed that there was in fact colocalization between the antibody and the microfibers.<sup>37</sup> HPLC–ESI–QTof–MS analysis showed that a few percent of the proteins in the microfibers were ones that interact with vimentin, namely, nestin, plectin, and lamin A.<sup>37</sup>

Figure 8B shows AFM images of fluorescent microfibers isolated from the cellular milieu. The peculiar morphology of these microfibers recalls the structure of the dimer of vimentin, representing the first level of vimentin self-assembly.<sup>40</sup> Figure 8C reports cell viability experiments showing that **5** is not toxic to B104 cells.

The ability to locate the fluorescent microfibers by LSCM and separate them from the cell lysate offers an unprecedented way to test their potential as innovative biomaterials. As shown in Figure 9, C2C12 myoblasts, B104 mouse neuroblastoma

cells, and NIH-3T3 mouse embryonic fibroblasts were seeded on collagen–**5** or vimentin–**5** fluorescent microfibers, and their behavior was monitored with time. After 48 h the cells assumed different morphologies and configurations depending on the microfibers on which they were seeded. After seeding on collagen–**5** microfibers, C2C12 myoblasts and B104 neuroblastoma cells (Figure 9Ae,Ag, respectively) displayed cytoskeleton remodeling with a remarkable organization of F-actin and a more elongated shape, whereas NIH-3T3 cells appeared to be spindle-shaped with a round and contracted cell body (Figure 9Af). By contrast, when seeded for 48 h on vimentin–**5** microfibers, 3T3 fibroblasts (Figure 9Bf) and B104 neuroblastoma cells (Figure 9Bg) maintained their polygonal shape with many actin cytoplasmic protrusions, while C2C12 myoblasts showed a contracted cell body (Figure 9Be). After 48 h of cell culture, the collagen–**5** and vimentin–**5** microfibers appeared as green fluorescent dots with a uniform distribution inside the cytoplasm of C2C12 myoblasts (Figure 9Ab,Bb) and NIH-3T3 fibroblasts (Figure 9Ac,Bc). In this case, both types of microfibers were degraded by the cells, conceivably by the





**Figure 8.** (A) LSCM images of the intracellular formation and growth of fluorescent microfibers with time upon spontaneous uptake of **5** by mouse neuroblastoma cells (B104 cell line). The inset in (c) shows the formation of helical microfibers. Scale bars: 50  $\mu\text{m}$ . (B) AFM images of fluorescent microfibers isolated from the cellular milieu. The arrows indicate the coiled coil arrangement of two smaller microfibers. (C) Cell viability tests. NT = nontreated cells; DTTO 5 = cells treated with compound **5**. Adapted with permission from ref 37. Copyright 2015 Royal Society of Chemistry.

action of matrix metalloproteases, modifying the microenvironment and resulting in an alteration of the cellular morphology and cytoskeleton rearrangement. On the contrary, in B104 neuroblastoma cells, collagen-**5** microfibers were partially degraded (Figure 9Ad) whereas the vimentin-**5** microfibers showed their native morphology (Figure 9Bd). It is likely that the degradation and possible recycling of the microfibers can be a process used to create the protein fragments required to build new cellular structures.

MTT proliferation assays on C2C12 myoblasts, 3T3 fibroblasts, and B104 neuroblastoma cells in the presence of collagen-**5** or vimentin-**5** microfibers showed that in no case did vimentin-**5** microfibers affect cell viability or proliferation, whereas collagen-**5** microfibers did not affect viability/proliferation only in the case of myoblasts and neuroblastoma cells.<sup>37</sup> Instead, the viability and proliferation of NIH-3T3 fibroblasts were badly compromised in the presence of NIH-3T3 physiologically secreted collagen-**5** microfibers. Our results indicate that the massive storage of collagen-**5** fragments inside fibroblasts leads to apoptosis. The biochemical mechanisms involved in the degradation of the fluorescent microfibers remains to be elucidated, but it is clear that the microfibers direct the behavior of seeded cells.

To our knowledge, the spontaneous uptake of biocompatible fluorescent and semiconducting dyes that can recognize specific intracellular proteins among the innumerable cell components and coassemble with them into functional biocompatible and biodegradable microfibers has not been described previously. Besides offering a new tool for the fluorescent imaging of biological processes, it opens a new research field that can be either alternative or complementary to current methods for the self-assembly of biomaterials.<sup>42–44</sup>

## SUMMARY AND PERSPECTIVES

We have described supramolecular microfibers spontaneously formed by oligothiophenes through two different assembly mechanisms in very different environments. The first, self-assembly of “sulfur-overrich” thiophene hexamers and octamers on surfaces, leads to thermodynamically stable fluorescent and conductive microfibers that, contrary to what is generally the case, can be grown on any type of surface with the same characteristics. The second, coassembly of oligothiophene-*S,S*-dioxides with specific fibrillar proteins inside live cells following a molecular recognition event, leads to the physiological formation of fluorescent and conductive oligothiophene-protein microfibers that are biocompatible, biodegradable, and not harmful to the cells. In both cases, the organization into microfibers enhances the properties of the molecular building blocks and enables new functionalities. In the first case, the assembly is promoted by multiple anisotropic nonbonding donor-acceptor intra- and intermolecular interactions that contribute to settling conformations and packing types. In the second case, it is the cell machinery that guides the coassembly process following a molecular recognition event between the oligothiophene and intracellular components of fibrillar proteins. What links together the two different microfiber types are the peculiar characteristics of the thiophene rings, namely, their geometric adaptability to the most various environments and the hypervalency of sulfur, both of which have been poorly exploited to date.

Can we foresee some kind of interfacing between the two different types of assembly described above? For example, could the use of smart oligothiophenes lead to the spontaneous assembly of optical and electronic devices inside live cells via the uptake of appropriate building blocks? Our answer to the

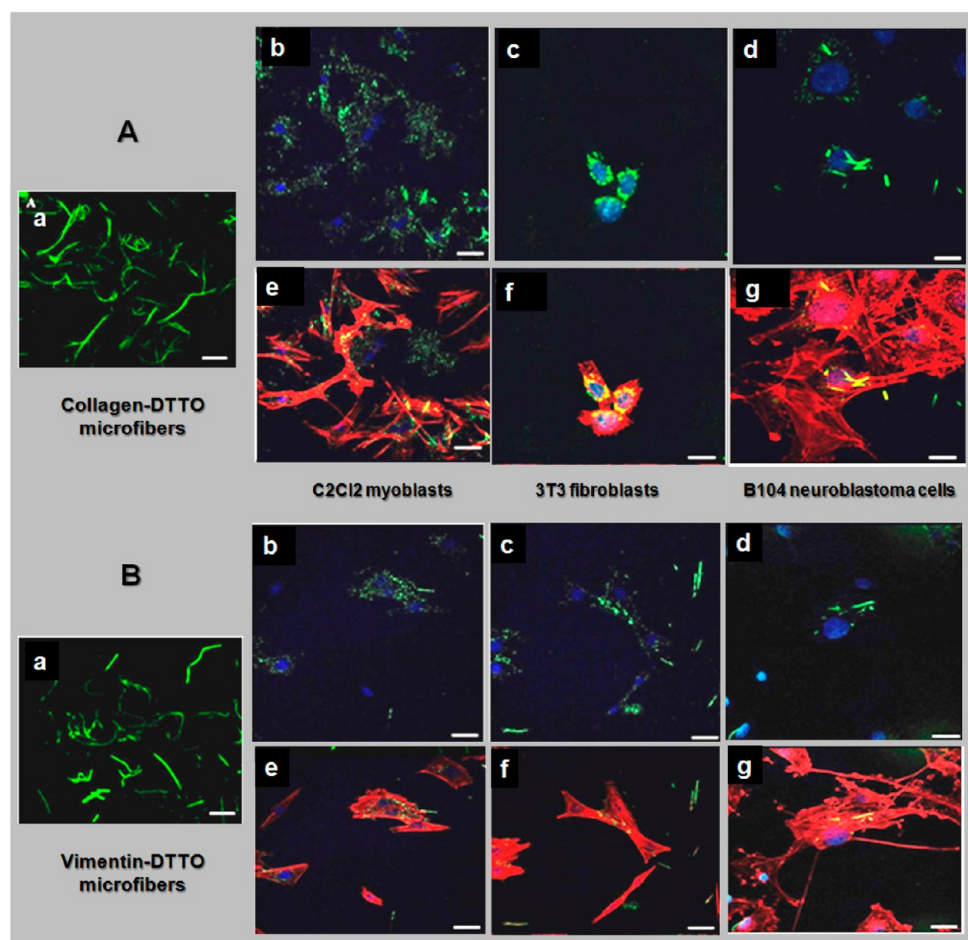


**Figure 9.** (Aa, Ba) LSCM images of the pristine collagen-5 and vimentin-5 microfibers, respectively, used as substrates for the deposition of live C2C12 myoblasts, 3T3 fibroblasts, and B104 neuroblastoma cells. After 48 h, the cells assumed different morphologies and configurations depending on the microfibers on which they were seeded. (Ab–g) LSCM images of fixed C2C12 myoblasts (b, e), 3T3 fibroblasts (c, f) and B104 neuroblastoma cells (d, g) seeded on collagen-5 microfibers for 48 h, stained with DAPI (blue, b–d) and actin (red, e–g). (Bb–g) Same as (Ab–g) for vimentin-5 microfibers. Scale bars: 10  $\mu$ m. Reproduced with permission from ref 37. Copyright 2015 Royal Society of Chemistry.

question is optimistic: yes, if we focus our attention on function-oriented synthesis<sup>45</sup> and take into account the great diversity of the chemical space.<sup>46</sup> Achieving the goal of spontaneous assembly of building blocks into operating devices inside cultured living cells would offer a useful model for basic investigations in many relevant fields such as tissue engineering, sensing, electrical control of biological function, monitoring of the electrical activity of neural cells, and so on. We hope that this Account encourages research leading toward the rational design of building blocks for new tools in this research area.

## AUTHOR INFORMATION

### Corresponding Author

\*E-mail: [giovanna.barbarella@isof.cnr.it](mailto:giovanna.barbarella@isof.cnr.it).

### Notes

The authors declare no competing financial interest.

### Biographies

**Giovanna Barbarella** received her Master in Chemistry from the University of Bologna (Italy) and her Ph.D. from the University of Grenoble (France) in 1974. After several years spent as research director at the Istituto per la Sintesi Organica e la Fotoreattività of the Italian National Research Council (ISOF-CNR), she is currently an associate researcher at ISOF. Her activity is focused on molecular

engineering of thiophene-based materials for applications in organic (opto)electronics and (bio)nanotechnology.

**Francesca Di Maria** received her Master in Chemistry from the University of Catania (Italy) in 2006 and at present is working on her Ph.D. thesis. Currently, her research activity is focused on the design and synthesis of conjugated materials in the framework of the project “MAAT-Molecular Nanotechnology to Human Health and the Environment” (PON02\_00563\_3316357) led by Prof. Giuseppe Gigli (University of Salento, Italy).

## ACKNOWLEDGMENTS

The authors are grateful for support by the Project “MAAT-Molecular Nanotechnology to Human Health and the Environment” (PON R & C 2007-2013, code PON02\_00563\_3316357).

## REFERENCES

- (1) Kim, F. S.; Ren, G.; Jenekhe, S. A. One-Dimensional Nanostructures of  $\pi$ -Conjugated Molecular Systems: Assembly, Properties, and Applications from Photovoltaics, Sensors, and Nanophotonics to Nanoelectronics. *Chem. Mater.* **2011**, *23*, 682–732.
- (2) Li, Y.; Liu, T.; Liu, H.; Tian, M. Z.; Li, Y. Self-Assembly of Intramolecular Charge-Transfer Compounds into Functional Molecular Systems. *Acc. Chem. Res.* **2014**, *47*, 1186–1198.

- (3) Mativetsky, J. M.; Orgiu, E.; Lieberwirth, I.; Pisula, W.; Samori, P. Charge Transport Over Multiple Length Scales in Supramolecular Fiber Transistors: Single Fiber Versus Ensemble Performance. *Adv. Mater.* **2014**, *26*, 430–435.
- (4) Xu, J.; Semin, S.; Niedzialek, D.; Kouwer, P. H. J.; Fron, E.; Coutino, E.; Savoini, M.; Li, Y.; Hofkens, J.; Uji-I, H.; Beljonne, D.; Rasing, T.; Rowan, A. E. Self-Assembled Organic Microfibers for Nonlinear Optics. *Adv. Mater.* **2013**, *25*, 2084–2089.
- (5) Hoeben, F. J. M.; Jonkheijm, P.; Meijer, E. W.; Schenning, A. P. H. J. About Supramolecular Assemblies of  $\pi$ -Conjugated Systems. *Chem. Rev.* **2005**, *105*, 1491–1546.
- (6) Aida, T.; Meijer, E. W.; Stupp, S. I. Functional Supramolecular Polymers. *Science* **2012**, *335*, 813–817.
- (7) Rasmussen, S. C.; Evenson, S. J.; McCausland, C. B. Fluorescent thiophene-based materials and their outlook for emissive applications. *Chem. Commun.* **2015**, *51*, 4528–4543.
- (8) Zhang, L.; Colella, N. S.; Cherniawski, B. P.; Mannsfeld, S. C. B.; Briseno, A. L. Oligothiophene Semiconductors: Synthesis, Characterization, and Applications for Organic Devices. *ACS Appl. Mater. Interfaces* **2014**, *6*, 5327–5343.
- (9) Schillinger, E. K.; Mena-Osteritz, E.; Hentschel, J.; Borner, H. G.; Bauerle, P. Oligothiophene Versus  $\beta$ -Sheet Peptide: Synthesis and Self-Assembly of an Organic Semiconductor-Peptide Hybrid. *Adv. Mater.* **2009**, *21*, 1562–1567.
- (10) Yagai, S.; Gushiken, M.; Karatsu, T.; Kitamura, A.; Kikkawa, Y. Rationally controlled helical organization of a multiple-hydrogen-bonding oligothiophene: guest-induced transition of helical-to-twisted ribbons. *Chem. Commun.* **2011**, *47*, 454–456.
- (11) Yagai, S.; Kinoshita, T.; Kikkawa, Y.; Karatsu, T.; Kitamura, A.; Honsho, Y.; Seki, S. Interconvertible Oligothiophene Nanorods and Nanotapes with High Charge-Carrier Mobilities. *Chem. - Eur. J.* **2009**, *15*, 9320–9324.
- (12) Barbarella, G.; Zambianchi, M.; Bongini, A.; Antolini, L. The Deformability of the Thiophene Ring: A Key to the Understanding of the Conformational Properties of Oligo- and Polythiophenes. *Adv. Mater.* **1993**, *5*, 834–838.
- (13) Diaz-Quijada, G. A.; Weinberg, N.; Holdcroft, S.; Pinto, B. M. Conformational Analysis of Oligothiophenes and Oligo(thienyl)furans by Use of a Combined Molecular Dynamics/NMR Spectroscopic Protocol. *J. Phys. Chem. A* **2002**, *106*, 1277–1285.
- (14) Marseglia, E. A.; Grepioni, F.; Tedesco, E.; Braga, D. Solid State Conformation and Crystal Packing of Methyl-Substituted Quaterthiophenes. *Mol. Cryst. Liq. Cryst. Sci. Technol., Sect. A* **2000**, *348*, 137–151.
- (15) Zauhar, R. J.; Colbert, C. L.; Morgan, R. S.; Welsh, W. J. Evidence for a Strong Sulfur-Aromatic Interaction Derived from Crystallographic Data. *Biopolymers* **2000**, *53*, 233–248.
- (16) Musher, J. I. The chemistry of hypervalent molecules. *Angew. Chem., Int. Ed. Engl.* **1969**, *8*, 54–68.
- (17) Gillespie, R. J.; Silvi, B. The octet rule and hypervalence: two misunderstood concepts. *Coord. Chem. Rev.* **2002**, *233–234*, 53–62.
- (18) Iwaoka, M.; Isozumi, N. Hypervalent Nonbonded Interactions of a Divalent Sulfur Atom. Implications in Protein Architecture and the Functions. *Molecules* **2012**, *17*, 7266–7283.
- (19) Dell, E. J.; Capozzi, B.; Xia, J.; Venkataraman, L.; Campos, L. M. Molecular length dictates the nature of charge carriers in single-molecule junctions of oxidized oligothiophenes. *Nat. Chem.* **2015**, *7*, 209–214.
- (20) Ghofraniha, N.; Viola, I.; Di Maria, F.; Barbarella, G.; Gigli, G.; Leuzzi, L.; Conti, C. Experimental evidence of replica symmetry breaking in random lasers. *Nat. Commun.* **2015**, *6*, 6058.
- (21) Barbarella, G.; Favaretto, L.; Sotgiu, G.; Antolini, L.; Gigli, G.; Cingolani, R.; Bongini, A. Rigid-Core Oligothiophene-S,S-dioxides with High Photoluminescence Efficiencies Both in Solution and in the Solid State. *Chem. Mater.* **2001**, *13*, 4112–4122.
- (22) Tedesco, E.; Della Sala, F.; Favaretto, L.; Barbarella, G.; Albesa-Jové, D.; Pisignano, D.; Gigli, G.; Cingolani, R.; Harris, K. D. M. Solid-State Supramolecular Organization, Established Directly from Powder Diffraction Data, and Photoluminescence Efficiency of Rigid-Core Oligothiophene-S,S-dioxides. *J. Am. Chem. Soc.* **2003**, *125*, 12277–12283.
- (23) Barbarella, G.; Melucci, M.; Sotgiu, G. The versatile thiophene: an overview of recent research on thiophene-based materials. *Adv. Mater.* **2005**, *17*, 1581–1593.
- (24) Di Maria, F.; Olivelli, P.; Gazzano, M.; Zanelli, A.; Biasiucci, M.; Gigli, G.; Gentili, D.; D'Angelo, P.; Cavallini, M.; Barbarella, G. A Successful Chemical Strategy To Induce Oligothiophene Self-Assembly into Fibers with Tunable Shape and Function. *J. Am. Chem. Soc.* **2011**, *133*, 8654–8661.
- (25) Palama, I.; Di Maria, F.; Viola, I.; Fabiano, E.; Gigli, G.; Bettini, C.; Barbarella, G. Live-Cell-Permeant Thiophene Fluorophores and Cell-Mediated Formation of Fluorescent Fibrils. *J. Am. Chem. Soc.* **2011**, *133*, 17777–17785.
- (26) Desiraju, G. R.; Nalini, V. Database Analysis of Crystal-structure-determining Interactions involving Sulphur: Implications for the Design of Organic Metals. *J. Mater. Chem.* **1991**, *1*, 201–203.
- (27) Gentili, D.; Di Maria, F.; Liscio, F.; Ferlauto, L.; Leonardi, F.; Maini, L.; Gazzano, M.; Milita, S.; Barbarella, G.; Cavallini, M. Targeting ordered oligothiophene fibers with enhanced functional properties by interplay of self-assembly and wet lithography. *J. Mater. Chem.* **2012**, *22*, 20852–20856.
- (28) Di Maria, F. Unpublished results.
- (29) Berger, R.; Butt, H. J.; Retschke, M. B.; Weber, S. A. L. Electrical Modes in Scanning Probe Microscopy. *Macromol. Rapid Commun.* **2009**, *30*, 1167–1178.
- (30) Di Maria, F.; Gazzano, M.; Zanelli, A.; Gigli, G.; Loiudice, A.; Rizzo, A.; Biasiucci, M.; Salatelli, E.; D'Angelo, P.; Barbarella, G. Synthesis and Photovoltaic Properties of Regioregular Head-to-Head Substituted Thiophene Hexadecamers. *Macromolecules* **2012**, *45*, 8284–8291.
- (31) Di Maria, F.; Fabiano, E.; Gentili, D.; Biasiucci, M.; Salzillo, T.; Bergamini, G.; Gazzano, M.; Zanelli, A.; Brillante, A.; Cavallini, M.; Della Sala, F.; Gigli, G.; Barbarella, G. Polymorphism in Crystalline Microfibers of Achiral Octithiophene: The Effect on Charge Transport, Supramolecular Chirality and Optical Properties. *Adv. Funct. Mater.* **2014**, *24*, 4943–4951.
- (32) Barbarella, G.; Zambianchi, M.; Ventola, A.; Fabiano, E.; Della Sala, F.; Gigli, G.; Anni, M.; Bolognesi, A.; Polito, L.; Naldi, M.; Capobianco, M. L. Bright oligothiophene N-succinimidyl esters for efficient fluorescent labeling of proteins and oligonucleotides. *Bioconjugate Chem.* **2006**, *17*, 58–67.
- (33) Capobianco, M. L.; Barbarella, G.; Manetto, A. Oligothiophenes as fluorescent markers for Biological Applications. *Molecules* **2012**, *17*, 910–933.
- (34) Zambianchi, M.; Di Maria, F.; Cazzato, A.; Gigli, G.; Piacenza, M.; Della Sala, F.; Barbarella, G. Microwave-Assisted Synthesis of Thiophene Fluorophores, Labeling and Multilabeling of Monoclonal Antibodies, and Long Lasting Staining of Fixed Cells. *J. Am. Chem. Soc.* **2009**, *131*, 10892–10900.
- (35) Di Maria, F.; Palamà, E.; Baroncini, M.; Barbieri, A.; Bongini, A.; Bizzarri, R.; Gigli, G.; Barbarella, G. Live cell cytoplasm staining and selective labeling of intracellular proteins by non-toxic cell-permeant thiophene fluorophores. *Org. Biomol. Chem.* **2014**, *12*, 1603–1610.
- (36) Viola, I.; Palamà, I. E.; Coluccia, A. M. L.; Biasiucci, M.; Dozza, B.; Lucarelli, E.; Di Maria, F.; Barbarella, G.; Gigli, G. Physiological formation of fluorescent and conductive protein microfibers in live fibroblasts upon spontaneous uptake of biocompatible fluorophores. *Integr. Biol.* **2013**, *5*, 1057–1066.
- (37) Palamà, I. E.; Di Maria, F.; D'Amone, S.; Barbarella, G.; Gigli, G. Biocompatible and biodegradable fluorescent microfibers physiologically secreted by live cells upon spontaneous uptake of thiophene fluorophore. *J. Mater. Chem. B* **2015**, *3*, 151–158.
- (38) Walter, A.; Gutknecht, J. Permeability of Small Nonelectrolytes through Lipid Bilayer Membranes. *J. Membr. Biol.* **1986**, *90*, 207–217.
- (39) Strasser, S.; Zink, A.; Janko, M.; Heckl, M.; Thalhammer, S. Structural investigations on native collagen type I fibrils using AFM. *Biochem. Biophys. Res. Commun.* **2007**, *354*, 27–32.

(40) Chernyatina, A. A.; Nicolet, S.; Aebi, U.; Herrmann, H.; Strelkov, S. V. Atomic structure of the vimentin central  $\alpha$ -helical domain and its implications for intermediate filament assembly. *Proc. Natl. Acad. Sci. U. S. A.* **2012**, *109*, 13620–13625.

(41) Goldie, K. N.; Wedig, T.; Mitra, A. K.; Aebi, U.; Herrmann, H.; Hoenger, A. Dissecting the 3-D structure of vimentin intermediate filaments by cryo-electron tomography. *J. Struct. Biol.* **2007**, *158*, 378–385.

(42) Tovar, J. D. Supramolecular Construction of Optoelectronic Biomaterials. *Acc. Chem. Res.* **2013**, *46*, 1527–1537.

(43) Wang, F.; Liu, Z.; Wang, B.; Feng, L.; Liu, L.; Lv, F.; Wang, Y.; Wang, S. Multi-Colored Fibers by Self-Assembly of DNA, Histone Proteins, and Cationic Conjugated Polymers. *Angew. Chem., Int. Ed.* **2014**, *53*, 424–428.

(44) Ko, J.; Mohtaram, N. K.; Ahmed, F.; Montgomery, A.; Carlson, M.; Lee, P. C. D.; Willerth, S. M.; Jun, M. B. G. Fabrication of poly (*ε*-caprolactone) microfiber scaffolds with varying topography and mechanical properties for stem cell-based tissue engineering Applications. *J. Biomater. Sci., Polym. Ed.* **2014**, *25*, 1–17.

(45) Wender, P. A.; Quiroz, R. V.; Stevens, M. C. Function through Synthesis-Informed Design. *Acc. Chem. Res.* **2015**, *48*, 752–760.

(46) Reymond, J. L. The Chemical Space Project. *Acc. Chem. Res.* **2015**, *48*, 722–730.